True double capture in collisions of bare and hydrogenlike ions with rare-gas atoms ($Z=7-13$)

S. Martin, J. Bernard, A. Denis, J. Désesquelles, and Li Chen
Laboratoire de Spectrométrie Ionique et Moléculaire, Université de Lyon 1, 43 boulevard du 11 Novembre 1918, F-69622 Villeurbanne Cedex, France

Y. Ouerdane
Laboratoire de Traitement du Signal et Instrumentation, Université de Saint-Etienne, 23 Rue du Dr. Paul Michelon, F-42023 Saint-Etienne, France

(Received 4 March 1994)

We measured relative cross sections for true double capture (TDC) and autoionizing double capture (ADC) in the collisions of slow bare Z^{Z+} and hydrogenlike $Z^{(Z-1)+}$ ions ($Z=7-13$) on rare gases. We found that the probabilities for radiative stabilization $P_{\rm rad}=\sigma_{\rm TDC}/(\sigma_{\rm TDC}+\sigma_{\rm ADC})$ are much stronger when the binding energies of the projectile captured electrons are comparable to those of the limits of the Rydberg $(3,n)$, $(4,n)$, and $(5,n)$ series. The observed strong effect of the projectile core on the probabilities for radiative stabilization of both electrons shows that the relaxation processes of the Rydberg electron play an important role.

PACS number(s): 34.70.+e, 34.50.Fa

I. INTRODUCTION

Electron capture into highly charged projectiles through collisions with target atoms has been studied extensively [1]. The overbarrier model [2] generally gives reliable predictions of final quantum states n, energy gain, and scattering angles for single capture processes, whereas angular momentum of the captured electron can be more accurately determined by using quasimolecular methods [3].

Concerning double electron capture, the situation is more intricate as electrons are generally captured into doubly excited states of which little is known concerning energies and autoionizing and radiative decay rates and which can interact with numerous $(nl,n'l')$ Rydberg series. As for single capture, an approach for understanding double electron capture is provided by the overbarrier model—an independent particle model—which predicts that emergent projectiles are populated in symmetrical or quasisymmetrical configurations ($n\cong n'$) in a sequential process [2]. Production of ions in these configurations was observed and their populations were measured by electron spectroscopy [4], proving that the doubly excited ions obtained by double electron capture decay at least partially through autoionization resulting in an autoionizing double capture (ADC) according to

$$A^{q+}+B\rightarrow A^{(q-2)+}(nl,n'l')+B^{2+}$$
$$\rightarrow A^{(q-1)+}(n''l'')+B^{2+}+e^{-}\ .$$

The capture followed by the stabilization of both electrons after radiative decay,

$$A^{q+}+B\rightarrow A^{(q-2)+}(nl,n'l')+B^{2+}$$
$$\rightarrow A^{(q-2)+}+h\nu+B^{2+}\ ,$$

called true double capture (TDC), is also possible. This stabilization of both electrons, without change of charge state, can be explained either by direct stabilization of symmetrical or quasisymmetrical electron configurations [5,6] or by stabilization after transfer to very asymmetrical configurations with a low-lying electron and a Rydberg electron ($n>10$).

Experimental evidence for direct stabilization has been given in energy gain measurements by Gaboriaud, Roncin, and Barat [7]. Using a photon-ion coincidence technique, we proved that the indirect stabilization via the asymmetrical Rydberg states is also present [8]. The population of asymmetrical configurations can be ascribed to an auto transfer to Rydberg states (ATR) from symmetrical or quasisymmetrical states. Bachau, Roncin, and Harel [9] proposed a post-collisional mechanism by which doubly excited (n,n) states, which are autoionizing at large internuclear distance, can be more strongly bound than the $n-1$ threshold while they are in the field of the recoil ion. During this time they can mix with more tightly bound ($n-1$, high n') states causing a loss of the high autoionizing probability of symmetrical states. Experimental signatures of the ATR process have been observed in O^{8+}-Ar and O^{8+}-He collisions by energy gain [7] and electron spectroscopy [10], where the $O^{6+}(4,4)$ population is transferred to the $O^{6+}(3l,n'l')$ Rydberg series. This transfer to an adjacent highly asymmetrical Rydberg series is induced by electron-electron interaction on the way out of the collision. Autoionization rates of these Rydberg states depend on the n' and l' quantum numbers. A large fraction of the $(3l,n'l')$ states can be stabilized for high n' and l' values. However, the manifolds have to be studied in detail and the properties of individual terms have to be considered separately, so that it is difficult to give rules for whole, symmetrical or asymmetrical, configuration manifold [11].

Ratios between direct and indirect stabilization depend

on the collision system. For N^{7+}-Kr collisions, direct stabilization is about 10% of total stabilization [7]. For Ne^{10+}-He, Bordenave *et al.* [12] found that the (4,4) levels are absent from the electron spectra and that only the $(3,n)$ Rydberg series is observed. Indirect stabilization can be determined by measuring the emission cross section of Rydberg transitions [13]. Total stabilization can be studied by charge state analysis of the reaction products [14–16]. An increase of the probability for a radiative stabilization with increasing projective charge has been found for $q>28$ in $Xe^{q+}+He$, Xe collisions by Cederquist *et al.* [16], for $q>9$ in $Ar^{q+}+Ar$ collisions, and for $q>12$ in $Kr^{q+}+Ar$ collisions by Ali *et al.* [17]. From this finding, they have concluded that the core structure of the projectile, rather than the initially populated doubly excited state, takes an important part in the electronic relaxation process. In this paper, we report measurements of probabilities for radiative stabilization for bare and hydrogenlike ions of charge state $q=7-13$ colliding on a rare gas target, and show that both parameters seem to play an important role. We attempt a qualitative explanation for the findings reported here.

II. EXPERIMENTAL SETUP

The experimental setup, shown in Fig. 1, has already been described [8,13], and only a brief account is presented here. The AIM (accélérateur d'ions multichargés) facility at Grenoble delivers mass- and energy-selected ion beams. Bare ions ($q=7-13$) and hydrogenlike ions ($q=6-13$) were extracted at an energy of $2q$ keV. After their passage through a 1-mm diaphragm, typical currents were a few electric nA for bare ions and much more for hydrogenlike ions (factor 5). The ion beam then intersects an effusive gas target. The scattered ions are analyzed by a parallel plate electrostatic analyzer and detected by a channeltron electron multiplier. A weak electric field extracts the recoil ions and a time of flight spectrometer is used to determine the charge state of recoil ions. For the best efficiency of detection, the recoil ions are accelerated at 5 kV just in front of the multichannel plate detector (MCP). The selected charge state of scattered ions detected by the channeltron provides the start pulse to the time to amplitude converter, which is stopped by the detection of a recoil ion. The time of flight of recoil ions are typically of a few microseconds. Typical background pressure in the target chamber is about 2×10^{-7} mbar, and gas injection pressures ranged from 0.05 to 0.5 mbar.

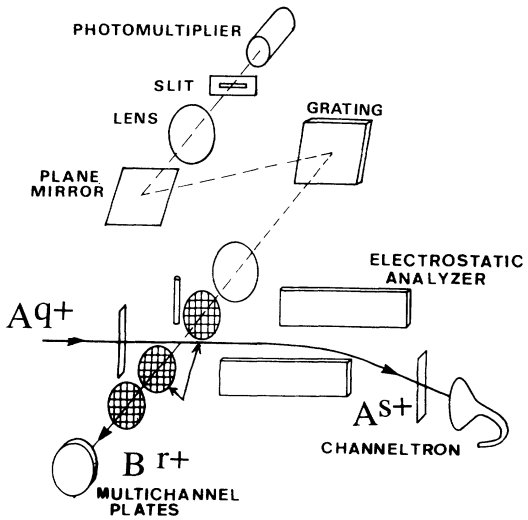

FIG. 1. Scheme of the experimental setup. A^{q+} incident ions, B^{r+} recoil ions, A^{s+} stabilized ions.

III. RESULTS AND DISCUSSION

Typical time of flight spectra are shown in Fig. 2 for Ne^{10+}-He collisions. The spectrum registered in coincidence with Ne^{9+} scattered ions is shown in Fig. 2(a). The He^{1+} peak is due to single-electron capture (SEC), and the He^{2+} peak results from autoionizing double capture (ADC). In the spectrum registered in coincidence with Ne^{8+} scattered ions [Fig. 2(b)], the He^{1+} peak is due exclusively to double collisions, and the He^{2+} one results mainly from true-double captures (TDC) with a small contribution from double collisions. The double collision contribution can be estimated with the method already described in detail [15]. A rough correction of this effect can be performed by substracting from the intensity of the measured TDC peak the ratio of ADC to SEC [Fig. 2(a)] multiplied by the intensity of the double collision peak [Fig. 2(b)]. A typical correction is about 5% of the TDC peak total intensity.

Table I gives the experimental data obtained for the radiative probabilities $P_{rad}=\sigma_{TDC}/(\sigma_{ADC}+\sigma_{TDC})$ and the ratios between total double capture and single capture

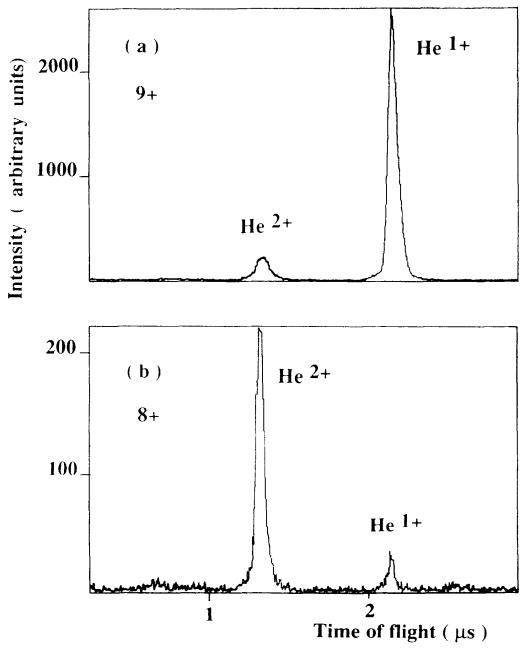

FIG. 2. Projectile-recoil ion coincidence spectra for Ne^{9+} (a) and Ne^{8+} (b) stabilized projectiles in Ne^{10+}-He collisions. The small peak produced by the Ne^{8+}-He^{+} coincidences in (b) is due to double collisions.

(DC to SEC) into bare ions ($Z=7-13$) for collisions on rare gas targets at $2Z$-keV energy. The values of E/Z^2, the double capture binding energy E predicted by the classical barrier model [2] divided by Z^2, are also given. The error bars for radiative probabilities are about 3% due to statistical errors and uncertainties in double collision correction. The error bars of about 5% for the DC to SEC ratio are due to the difficulties in estimating the relative detection efficiencies of the MCP detector for B^{1+} and B^{2+} recoil ions. Figure 3 presents the measured radiative probabilities as a function of the (E/Z^2) energy. The energy diagram of the $(3,n)$, $(4,n)$, $(5,n)$, $(6,n)$, and $(7,n)$ doubly excited states of Ne IX is displayed in Fig. 4. The main features of the energy diagrams of other heliumlike ions ($Z=7-13$) are practically identical with the Ne IX diagram. Thus Fig. 4 applies to other projectiles after multiplying the Ne energy values by $Z^2/100$. Calculations of the (4,4) manifold energies for $Z=7-10$ ions can be found in Ref. [18]. Since the number of states within each manifold is quite large, only the lowest and the highest levels are traced. The ionization thresholds of

TABLE I. Radiative probabilities P_{rad} for bare ion on rare gas target collisions. DC to SEC is the ratio between total double capture and single capture. E/Z^2 is the double capture binding energies divided by Z^2. Collision energies are $2Z$ keV.

Collision	P_{rad} (%)	DC to SEC (%)	$100E/Z^2$ (eV)
$N^{7+}+He$	<5	19	261.4
$N^{7+}+Ne$	5	48	208.2
$N^{7+}+Ar$	35	39	145
$N^{7+}+Kr$	40	53	128.2
$N^{7+}+Xe$	27	71	111.4
$O^{8+}+He$	10	37	210.4
$O^{8+}+Ne$	11	40	167.7
$O^{8+}+Ar$	28	51	116.7
$O^{8+}+Kr$	22	57	103.2
$O^{8+}+Xe$	28	75	89.7
$F^{9+}+He$	17	24	173.7
$F^{9+}+Ne$	41	33	138.4
$F^{9+}+Ar$	17	41	96.4
$F^{9+}+Kr$	34	40	85.3
$F^{9+}+Xe$	37	56	74.1
$Ne^{10+}+He$	48	20	146.4
$Ne^{10+}+Ne$	18	43	116.7
$Ne^{10+}+Ar$	42	52	81.3
$Ne^{10+}+Kr$	36	60	71.9
$Ne^{10+}+Xe$	17	60	62.5
$Na^{11+}+Ne$	12	38	100
$Na^{11+}+Ar$	31	33	69.7
$Na^{11+}+Kr$	14	52	61.6
$Na^{11+}+Xe$	19	60	53.6
$Al^{13+}+Ne$	52	35	76.3
$Al^{13+}+Ar$	21	44	53.1
$Al^{13+}+Kr$	19	39	47
$Al^{13+}+Xe$	9	70	40.9

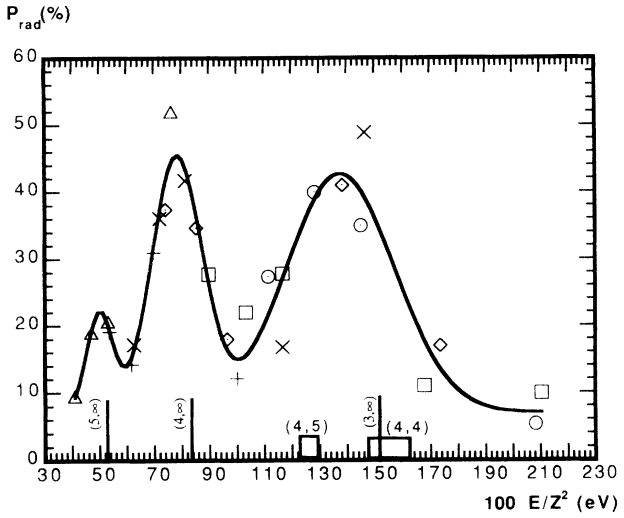

FIG. 3. The probabilities for radiative stabilization, P_{rad}, for bare incident projectiles, as a function of the double capture binding energies predicted by the classical barrier model multiplied by $100/Z^2$. Error bars are about three percent. (○, nitrogen; □, oxygen; ◇, fluorine; ×, neon; +, sodium; △, aluminum). For each ion, the first point at low energy corresponds to a Xe target, the second one to a Kr target, and so on for Ar, Ne, and He.

Ne X are represented by black lines. We note that the (4,4) manifold overlaps with $(3,n)$ configurations ($n=10,\infty$), and the (5,5) and (5,6) manifolds overlap with $(4,n)$ configurations.

In Fig. 3, the limits of each series $n=3$, 4, and 5 of Ne IX ions are indicated by means of three vertical lines, and the positions of the (4,4), (4,5) manifolds by means of rectangles along the abscisse axis. The considerable variations of the radiative probabilities, from 5% to 40% in

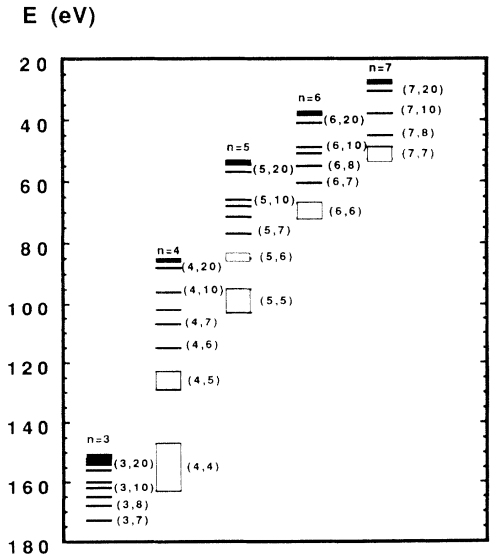

FIG. 4. Energy-level diagram of doubly excited states of Ne IX. The black lines represent the one-electron ionization thresholds. We have indicated only a few Rydberg levels.

the $n=3$ limit vicinity, from 10% to 40% around the $n=4$ limit, and from the 10% to 20% around the $n=5$ limit, are remarkable. These measurements strongly suggest that the TDC process is related to the population of asymmetrical Rydberg states near the ionization limits. This estimation is justified in other ways by optical spectral observations. In fact, for collision systems with high measured value of P_{rad}, we have observed high intensities of optical transitions from $(3,n)$ and $(4,n)$ Rydberg configurations. It is not surprising that asymmetrical Rydberg states contribute to radiative rates, since the interaction between the electrons depends on their respective binding energies. For a given internal electron state, the higher the n and l values of the Rydberg electron, the weaker the repulsive force between them. Consequently the autoionization of $(3,n)$ and $(4,n)$ asymmetrical configurations is much lower than that of quasisymmetrical configurations.

We have already noted that peaks of P_{rad} were observed in the vicinity of the series limits, but they are not exactly centered on them, being slightly shifted toward lower binding energies, as is well evidenced for the $n=3$ peak. Let us try to understand these findings by comparing the O^{8+}-Ar and N^{7+}-Ar systems. Gaboriaud, Roncin, and Barat [7], using energy gain measurements, have shown that for O^{8+}-Ar collisions the stabilization can go through the quasisymmetrical configuration (4,5). They found that the initial populations relative to the total double capture are 29% for (4,4) and 71% for (4,5) configurations and that the stabilization ratios relative to capture into each configuration are 59% for (4,4) and 11% for (4,5). Thus the high radiative probability measured for this system is partially due to direct stabilization of (4,5) configurations shifting the "$n=3$ peak" toward the (4,5) manifold, i.e., toward lower binding energies as seen in Fig. 3. As for N^{7+}-Ar collisions, the initial population is almost entirely in the (4,4) manifold. However, we measured a 34% radiative stabilization, a much smaller ratio than for O^{8+}-Ar collisions (59%), which shows that the (4,4) manifold is populated differently depending on the collision systems. Based on the ATR mechanism, we could interpret the difference in stabilization ratios of the (4,4) manifold by the fact that, in N^{7+}-Ar collisions, lower Rydberg $(3,n)$ states might be populated than in O^{8+}-Ar collisions. An important part of these (3, low n) configurations can autoionize, because the autoionization rate increases rapidly as n decreases. Far from the "$n=3$ peak," at higher binding energies, low but not zero radiative probabilities were found, suggesting the possibility of direct population of (3,5) and (3,6) levels. Forthcoming measurements of the Rydberg transition decay of various collision systems will allow us to learn the $(3,n)$ initial population distributions.

For collision systems in the vicinity of the $(4,\infty)$ limit, few experimental studies have been reported, and a peak similar to that of the $(3,\infty)$ limit is observed. The $(4,\infty)$ limit is near the quasisymmetrical configurations (5,6) which probably populate $(4,n)$ Rydberg states by the auto-transfer process, as in the case of (4,4) to $(3,n)$. The peak near the $(5,\infty)$ limit is less important. We notice from the energy diagram that the $(5,n)$ Rydberg states overlap the two $(6,n')$ and $(7,n'')$ series, which suggests a more complicated process for populating $(5,n)$ than in $(3,n)$ and $(4,n)$ Rydberg states.

Radiative probabilities for incident hydrogenlike ions ($q=6-13$) were measured to be about three times lower than for bare ions. This is the first signature of a core effect on P_{rad}. This lower value is probably due to the removing of the l degeneracy of the $1s3snl$, $1s3pnl$, and $1s3dnl$ Rydberg series of lithiumlike ions. In the case of Na X, calculations using a MCDF computer code [19] give 156.03-, 153.12-, and 151.36-eV binding energies for the $1s3s$, $1s3p$, and $1s3d$ states, respectively. Thus the $1s3dnl$ states of Na IX can autoionize to $1s3p$ and $1s3s$ opened channels when the Rydberg states are higher than $n=25$ and 16, respectively. For Na IX $1s3pnl$ states, the limit is $n=20$. The radiative emission probabilities of the Na IX $1s3lnl'$ levels have been approximated by the probabilities for the core Na X $1s3l$ by extrapolating values known in the helium sequence [20]. They are 2.3×10^{11} s^{-1}, 4.0×10^{12} s^{-1}, and 6.4×10^{11} s^{-1} for $3s$, $3p$, and $3d$, respectively. As for the autoionization probabilities of $1s3lnl$ levels, Poirier's calculations [21] show that only the Rydberg states with low angular momentum ($l<7$) can autoionize on the $3l$ continuum. We conclude that the l distribution of the Rydberg electron plays an important role in the stabilization of two electrons for collisions using hydrogenlike ions.

For bare ions, and for hydrogenlike ones as well, a better understanding of the stabilization of both captured electrons would require more calculations for radiative and autoionizing probabilities and more data on the distribution of the Rydberg state l-level populations. Experiments using coincidences between ions and photons in a wider range, including the UV light from low and intermediate angular momentum states, might be able to provide important information about these processes.

ACKNOWLEDGMENTS

The authors are grateful to M. Poirier and P. Roncin for helpful and valuable discussions, and to T. Lamy, A. Brenac, and G. Lamboley for their assistance in running the ECR ion source and the AIM accelerator. AIM is a joint CEA-CNRS facility. The Laboratoire de Spectrométrie Ionique et Moléculaire is "Unité Associée au Centre National de la Recherche Scientifique No. 171."

[1] K. Janev and H. Winter, Phys. Rep. **117**, 265 (1985).
[2] A. Niehaus, J. Phys. B **19**, 2925 (1986).
[3] C. Harel and H. Jouin, Europhys. Lett. **11**, 121 (1990).
[4] P. Benoit-Cattin, A. Bordenave-Montesquieu, M. Boudjema, A. Gleizes, S. Dousson, and D. Hitz. J. Phys. B **21**, 3387 (1988).
[5] N. Vaeck and J. E. Hansen, J. Phys. B **25**, 3267 (1992); **26**, 2977 (1993).
[6] Z. Chen and C. D. Lin, J. Phys. B **26**, 957 (1993).
[7] M. N. Gaboriaud, P. Roncin, and M. Barat, J. Phys. B **26**, L303 (1939).
[8] S. Martin, A. Denis, Y. Ouerdane, and M. Carré, Phys. Lett. A **165**, (1992); **165**, 441 (1992).
[9] H. Bachau, P. Roncin, and C. Harel, J. Phys. B **25**, L109 (1992).
[10] M. Boudjema, P. Moretto-Capelle, A. Bordenave-Montesquieu, P. Benoit-Cattin, A. Gleizes, H. Bachau, P. Galan, F. Martin, A. Riera, and M. Yanez, J. Phys. B **22**, L121 (1989); P. Moretto-Capelle *et al.*, *ibid.* **22**, 271 (1989).
[11] N. Vaeck and J. E. Hansen, J. Phys. B **26**, 2977 (1993).
[12] A. Bordenave-Montesquieu, P. Moretto-Capelle, A. Gonzalez, M. Benhenni, and H. Bachau, J. Phys. B (to be published).
[13] S. Martin, A. Denis, A. Delon, J. Désesquelles, and Y. Ouerdane, Phys. Rev. A **48**, 1171 (1993).
[14] L. Guillemot, P. Roncin, M. N. Gaboriaud, H. Laurent, and M. Barat, J. Phys. B **23**, 4293 (1990).
[15] A. Delon, S. Martin, A. Denis, Y. Ouerdane, M. Carré, J. Désesquelles, and M. C. Buchet-Poulizac, Radiat. Eff. Defects Solids **126**, 337 (1993).
[16] H. Cederquist, H. Andersson, E. Beebe, C. Biedermann, L. Broström, A. Engström, H. Gao, R. Hutton, J. C. Levin, L. Liljeby, M. Pajek, T. Quinteros, N. Selberg, and P. Sigray, Phys. Rev. A **46**, 2592 (1992).
[17] R. Ali, C. L. Cocke, M. L. A. Raphaelian, and M. Stockli, J. Phys. B **26**, L177 (1993).
[18] H. Bachau, C. Harel, M. Barat, P. Roncin, A. Bordenave-Montesquieu, P. Moretto-Capelle, P. Benoit-Cattin, A. Gleizes, and M. Benhenni, in *The Physics of Highly Charged Ions,* Proceedings of the VIth International Conference on the Physics of Highly Charged Ions, edited by P. Richard, M. Stockli, C. L. Cocke, and C. D. Lin, AIP Conf. Proc. No. 274 (AIP, New York, 1992); H. Bachau, J. Phys. B **17**, 1771 (1984).
[19] J. P. Desclaux, Comput. Phys. Commun. **9**, 31 (1975).
[20] N. M. Cann and A. J. Thakkar, Phys. Rev. A **46**, 5397 (1992).
[21] M. Poirier, Phys. Rev. A **38**, 3484 (1988), and (private communication).